Structural Engineering and Mechanics, *Vol. 64, No. 3 (2017) 293-299*
DOI: https://doi.org/10.12989/sem.2017.64.3.293

Theoretical evaluation of collision safety for Submerged Floating Railway Tunnel (SFRT) by using simplified analysis

Sung-il Seo[1a], Jiho Moon[*2] and Hyung-Suk Mun[1b]

[1]*New Transportation Research Center, Korea Railroad Research Institute(KRRI), Uiwang-Si, Gyeonggi-do, 437-757, South Korea*
[2]*Department of Civil Engineering, Kangwon National University, Chuncheon-si, Gangwon-do 24341, South Korea*

(Received June 14, 2016, Revised July 4, 2017, Accepted July 11, 2017)

Abstract. Submarine collisions is one of the major hazardous factor for Submerged Floating Railway Tunnel (SFRT) and this study presents the safety evaluation for submarine collision to SFRT by using theoretical approach. Simplified method to evaluate the collision safety of SFRT was proposed based on the beam on elastic foundation theory. Firstly, the time history load function for submarine collision was obtained by using one-degree-of-freedom vibration model. Then, the equivalent mass and stiffness of the structure were calculated, and the collision responses of SFRT were evaluated. Finite element analysis was conducted to verify the proposed equations, and it can be found that the collision responses, such as deflection, and acceleration, agreed well with the proposed equations. Finally, derailment condition for high speed train in SFRT due to submarine collision was proposed.

Keywords: Submerged Floating Railway Tunnel (SFRT); submarine collision; collision analysis

1. Introduction

Fig. 1 shows the concept of Submerged Floating Railway Tunnel (SFRT). SFRT is supported by buoyancy in the water and it can be constructed easily regardless of the water depth, while construction efficiency is dramatically decreased with increasing water depth for immersed or subsea tunnel. SFRT consists of a series of tubular segments. The segments are constructed on the land, and SFRT can be completed by connecting the segments on the water. Therefore, construction time and cost can be considerably reduced comparing to the immersed or subsea tunnel (Østlid 2010). SFRT is quite stable structure system since external forces generated by winds and waves are significantly reduced by increasing the submergence depth. For SFRT, buoyancy is generally larger than gravity load and it tends to come up to the surface. This up-lift force is balanced by the tension forces in mooring lines.

The concept of Submerged Floating Tunnel (SFT) was first proposed in 1,880s and some feasible studies have been reported (Østlid 2010, Kanie 2010). In Italy and Japan, basic designs of SFTs have been conducted. China is in the process of SFT project to cross the lake. However, there is no real construction case in the world yet (Mazzolani *et al.* 2010). There are several reasons why real construction of SFRT is hard. One of major obstacle is passenger's concerns about evacuation in emergency situation, since SFRT is in deep water. Thus, it is necessary to ensure high safety level in emergency situation and to provide the safety of passenger for real application of SFRT.

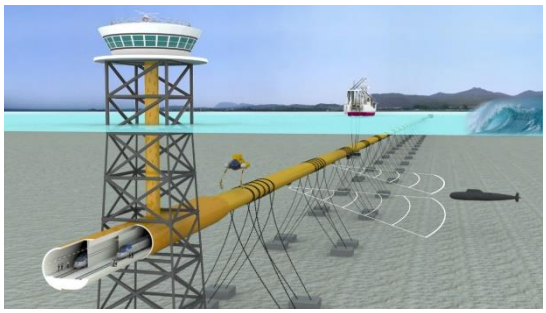

Fig. 1 Concept of Submerged Floating Railway Tunnel (SFRT)

There are several emergency cases in SFRT such as a leakage of water and mooring line breakdown. One of important hazardous factor is a collision with third object such as submarine and floating vessel. When SFRT is located more than 20 m below the water level, there are little chance of collision with floating vessel. Even if, collision with submarine may be prevented by using proper alarm facilities such as sonar, the safety of SFRT must be verified for the worst case scenario of the collision with submarine, such as drifting of submarine, malfunction of alarm device, and etc.

Some collision analysis methods for SFT are suggested by previous researchers. Zhang *et al.* (2010) calculated the maximum deflection of Qiandao Lake SFT by using energy conservation theorem where only bending moment of the beam is considered neglecting the effect of mooring lines. Hong and Lee (2014) analyzed SFT subjected to collision

∗Corresponding author, Assistant Professor
E-mail: jmoon1979@kangwon.ac.kr
[a]Senior Principal Researcher
E-mail: siseo@krri.re.kr
[b]Principal Researcher
E-mail: hsmun@krri.re.kr

ISSN: 1225-4568 (Print), 1598-6217 (Online)

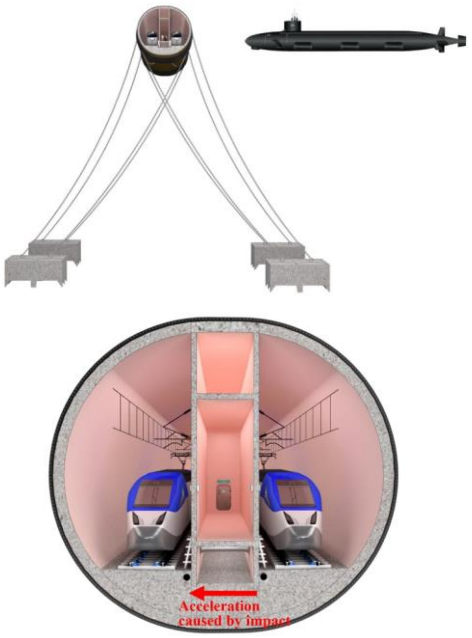

Fig. 2 SFRT under submarine collision and section of SFRT

load by using commercial finite element analysis code. Generally, complex responses due to collision can be simulated by three dimensional finite element analysis. However, it is somewhat time consuming procedure and simplified analysis method to identify the collision characteristic is needed in the preliminary design stage (Seo and Kim 2012). For the problem of collision of floating vessel with other structures, several researches have been conducted (Consolazio *et al.* 2005) and design guide line has been provided (DNV 2010). For example, for the collision of floating vessel with bridge pier in offshore, design code to verify the safety of the bridge pier is provided in AAHSTO design guide (2009). However, such research is very limited for SFRT.

In this study, collision safety of SFRT was evaluated by using theoretical approach. Simplified analysis method for collision with submarine was proposed and it was verified by comparing with the results of finite element analysis. Further, derailment condition for high speed train in SFRT due to submarine collision was also proposed. By using the proposed analysis method, impact responses of SFRT and stability of the train under submarine collision can be simply checked in the preliminary design stage.

2. Theoretical evaluation of collision behavior for SFRT

2.1 displacement and acceleration

Fig. 2 shows SFRT considered in this study. SFRT has a pipeline structure where inner space is large enough to pass two high speed trains. The cross section is the double skinned concrete composite structures where outer and inner shells are made of steel and concrete is filled inside. The buoyancy of SFRT is in the equilibrium state by tension

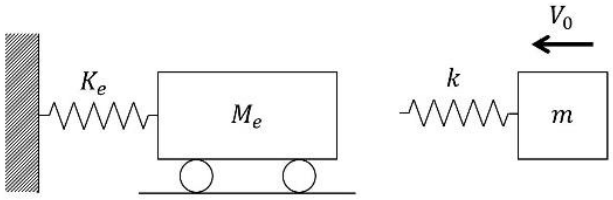

Fig. 3 1 degree of freedom mass-spring model for SFRT under submarine collision

forces in mooring lines. Mooring lines are equally spaced and they are anchored to the ground by gravity of concrete block, as shown in Fig. 2.

Fig. 3 shows mass-spring model simulating collision of SFRT with submarine. SFRT is modeled as 1 degree of freedom mass-spring system having equivalent mass, M_e, and equivalent stiffness, K_e. It is assumed that submarine has constant initial velocity, V_0, where mass and stiffness of submarine are equal to m and k, respectively. From the view point of structural design, the maximum response of the system is more important than time history behavior. Thus, the effect of damping on the maximum response is negligible and the damping is not considered in this study for simplicity of the problem. The equation of motion for submarine neglecting damping is given by

$$m\ddot{x} + kx = 0 \tag{1}$$

where x is displacement in horizontal direction. For the collision problem described in Fig. 3, only compression is transferred to SFRT by collision of submarine. For the particle having initial velocity of V_0, the solution of Eq. (1) is given by

$$x = \frac{V_0 t_d}{\pi} \sin\frac{\pi}{t_d} t, \qquad \text{where } t_d = \pi\sqrt{\frac{m}{k}} \tag{2}$$

The reaction force (or impact force) generated by collision can be simply calculated by multiplying stiffness of submarine, k, to Eq. (2). Thus, the maximum reaction force, $F_{\max}$, can be obtained by

$$F_{max} = kx_{max} = V_0\sqrt{mk} \tag{3}$$

where $x_{\max}$ is the maximum displacement of the submarine. It should be noted that the displacement shown in Eq. (1) has sinusoidal shape. However, only compressive force is effective for the collision. Thus, impact load due to submarine collision has half sine shape, as shown in Fig. 4 assuming SFRT and submarine don't contact after first collision.

The equation of motion for SFRT subjected to impact load can be written as

$$M_e\ddot{x} + K_e x = F(t) \tag{4}$$

where M_e and K_e are equivalent mass including added virtual mass and stiffness of SFRT, respectively. $F(t) = F_{max}\sin\omega_d t$ when $0 \le t < t_d$, and $F(t) = 0$ when $t \ge t_d$. The solution of Eq. (4) is given by

$$x = \frac{F_{max}\omega}{K_e(\omega_d^2 - \omega^2)}[-\omega\sin\omega_d t + \omega_d \sin\omega t], \quad \text{when } 0 \le t < t_d \tag{5}$$

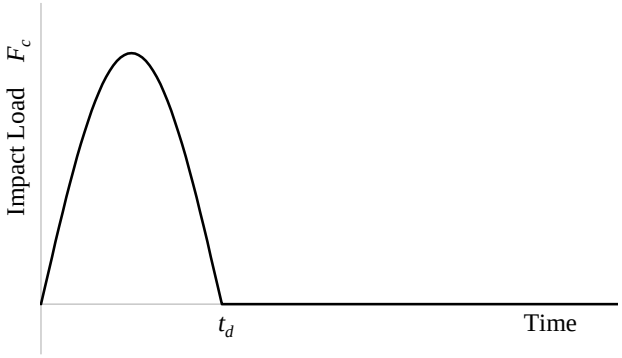

Fig. 4 Time history of impact load

$$x = \frac{F_{max}\omega\omega_d}{K_e(\omega_d^2-\omega^2)}[\sin\omega(t-t_d) + \sin\omega t], \quad \text{when } t \geq t_d \tag{6}$$

In Eqs. (5)-(6), ω is the natural frequency of SFRT, and it is given by $\omega = \sqrt{K_e/M_e}$. $\omega_d = \pi/t_d$ and it represents the exiting frequency of the load. Second differentiation of Eqs. (5)-(6) represent the acceleration of SFRT. Thus, acceleration, *a*, can be obtained as

$$a = \ddot{x} = \frac{F_{max}}{K_e}\frac{\omega^2}{(\omega_d^2-\omega^2)}[\omega_d^2 \sin\omega_d t - \omega\omega_d \sin\omega t], \quad \text{when } 0 \leq t < t_d \tag{7}$$

$$a = \ddot{x} = -\frac{F_{max}}{K_e}\frac{\omega^2}{(\omega_d^2-\omega^2)}\omega\omega_d[\sin\omega(t-t_d) + \sin\omega t], \text{ when } t \geq t_d \tag{8}$$

To solve Eqs. (5)-(8), equivalent mass and stiffness of SFRT have to be quantified firstly. SFRT is continuously supported by mooring lines in the water. Thus, SFRT can be simulated by beam on elastic foundation. In this study, equivalent mass and stiffness of SFRT is derived based on beam on elastic foundation theory and the details are described in next section.

2.2 Equivalent mass and stiffness

The equivalent mass, M_e, of SFRT can be obtained by using the concept of displacement function, and M_e is given by

$$M_e = \int_{-\infty}^{\infty} m_s\varphi(x)^2 dx \tag{9}$$

where m_s is the mass per unit length including added mass and $\varphi(x)$ is the displacement function.

As mentioned before, SFRT is continuously supported by mooring lines and it can be idealized by beam on elastic foundation, as shown in Fig. 5. For beam on elastic foundation subjected to the concentrated load, the deflection and bending moment of the beam can be expressed as (Ugural and Fenster 2012)

$$w(x) = \frac{P}{2\alpha k_s}e^{-\frac{x}{\alpha}}\left(\cos\frac{x}{\alpha} + \sin\frac{x}{\alpha}\right) = \frac{P}{2\alpha k_s}\varphi(x) \tag{10}$$

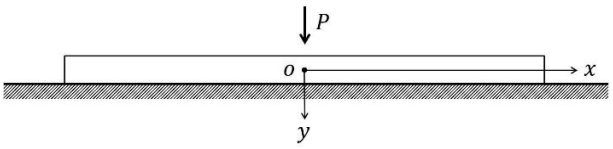

Fig. 5 Beam on elastic foundation subjected to central concentrated load

$$B_M(x) = EI\frac{d^2w(x)}{dx^2} = \frac{P}{2\alpha k_s}\frac{d^2\varphi(x)}{dx^2} = EI\frac{P}{k_s}\left(\frac{1}{\alpha}\right)^3 e^{-\frac{x}{\alpha}}\left(-\cos\frac{x}{\alpha} + \sin\frac{x}{\alpha}\right) \tag{11}$$

In Eqs. (10)-(11), *w(x)* and $B_M(x)$ represent the deflection and bending moment of the beam, respectively. α is the effective length of the beam and it is equal to $(4EI/k_s)^{1/4}$ where *EI* and k_s is the flexural stiffness of the beam and stiffness of the elastic foundation, respectively. From Eq. (10), $\varphi(x)$ is given by

$$\varphi(x) = e^{-\frac{x}{\alpha}}\left(\cos\frac{x}{\alpha} + \sin\frac{x}{\alpha}\right) \tag{12}$$

Thus, by substituting Eq. (12) into Eq. (9), M_e at the point of impact, where x=0, can be obtained as

$$M_e = 2\int_0^{\infty} m_s[e^{-\frac{x}{\alpha}}\left(\cos\frac{x}{\alpha} + \sin\frac{x}{\alpha}\right)]^2 dx = \frac{3}{2}m_s\alpha \tag{13}$$

and equivalent stiffness, K_e, at impact point (x=0) can be given by

$$K_e = \frac{P}{w(0)} = 2k_s\alpha \tag{14}$$

2.3 Impact responses

Impact responses of SFRT can be obtained by using Eqs. (5) and (6) with equivalent mass and stiffness shown in Eqs. (13) and (14). By using these equations, dimensionless displacement of SFRT can be written as

$$D_r = \frac{x}{\frac{F_{max}}{K_e}\frac{\omega}{\omega_d}} = \frac{1}{\left[1-\left(\frac{\omega}{\omega_d}\right)^2\right]}\left[-\frac{\omega}{\omega_d}\sin\frac{\omega t}{\frac{\omega}{\omega_d}} + \sin\omega t\right] \text{ and} \tag{15}$$

$$D_{rmax} \cong 2 \text{ when } 0 \leq \omega t < \frac{\omega}{\omega_d}\pi. \tag{16}$$

$$D_r = \frac{2}{\left[1-\left(\frac{\omega}{\omega_d}\right)^2\right]}\sin\left(\omega t - \frac{\omega}{\omega_d}\frac{\pi}{2}\right)\cos\left(\frac{\omega}{\omega_d}\frac{\pi}{2}\right) \text{ and} \tag{17}$$

$$D_{rmax} = \frac{2}{\left[1-\left(\frac{\omega}{\omega_d}\right)^2\right]}\cos\frac{\omega}{\omega_d}\frac{\pi}{2} \text{ when } \omega t \geq \frac{\omega}{\omega_d}\pi. \tag{18}$$

In Eqs. (15)-(18), D_r and D_{rmax} is the dimensionless displacement and the maximum dimensionless displacement, respectively. Fig. 6 shows variations in D_r with ωt for various frequency ratios ω/ω_d. From Fig. 6, it can be found that D_r is shifted to the left and converged to D_r =2 with decreasing ω/ω_d ratio.

Based on Eqs. (7) and (8), dimensionless acceleration of

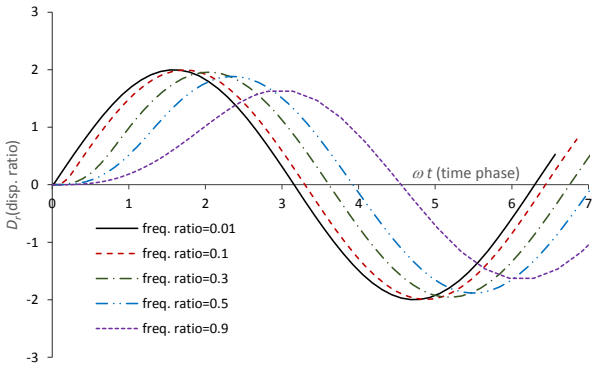

Fig. 6 Time history of D_r for various ω/ω_d

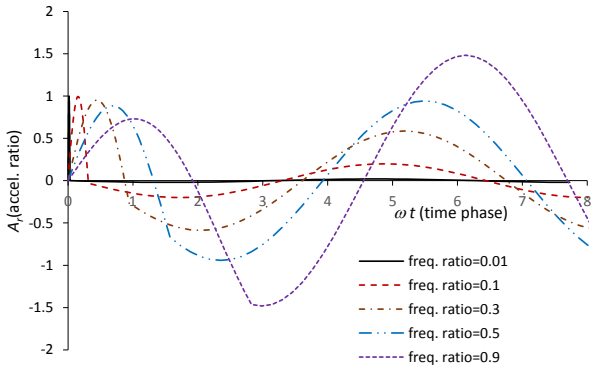

Fig. 7 Time history of A_r for various ω/ω_d

SFRT can be obtained as

$$A_r = \frac{a}{\frac{F_{max}}{K_e}\omega^2} = \frac{1}{1-\left(\frac{\omega}{\omega_d}\right)^2}\left[sin\frac{\omega t}{\frac{\omega}{\omega_d}} - \frac{\omega}{\omega_d} sin\,\omega t\right] \quad \text{and} \tag{19}$$

$$A_{rmax} \cong 1 \quad \text{when} \quad 0 \le \omega t < \frac{\omega}{\omega_d}\pi. \tag{20}$$

$$A_r = -\frac{2}{1-\left(\frac{\omega}{\omega_d}\right)^2}\frac{\omega}{\omega_d} sin\left(\omega t - \frac{\omega}{\omega_d}\frac{\pi}{2}\right) cos\left(\frac{\omega}{\omega_d}\frac{\pi}{2}\right) \quad \text{and} \tag{21}$$

$$A_{rmax} = \frac{2}{1-\left(\frac{\omega}{\omega_d}\right)^2}\frac{\omega}{\omega_d} cos\left(\frac{\omega}{\omega_d}\frac{\pi}{2}\right) \quad \text{when} \quad \omega t \ge \frac{\omega}{\omega_d}\pi. \tag{22}$$

In Eqs. (19)-(22), A_r is the dimensionless acceleration and A_{rmax} represents the maximum dimensionless acceleration. Variations in A_r with ωt for various ω/ω_d ratios are shown in Fig. 7. It is found that A_r is converged to one with deceasing ω/ω_d ratio. Generally, natural frequency of SFRT is considerably smaller than exiting frequency and $\omega/\omega_d \cong 0$. Thus, SFRT has constant A_{rmax} of one.

2.4 Maximum impact load and duration

The maximum impact load of submarine is expressed by Eq. (3) in previous section 2.1. However, stiffness of submarine, *k*, must be known to use Eq. (3). When there is no information about stiffness of submarine, *k*, alternative method to determine the maximum impact load of submarine has to be used. AASHTO (2009) suggested the design guide for collision of floating vessel to bridge. According to AASHTO (2009), the maximum impact load

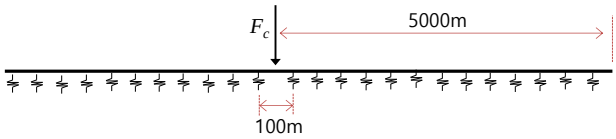

Fig. 8 Finite element model for SFRT subjected to central impact load

of floating vessel is given by

$$F_{max} = 119V_0\sqrt{D_{WT}} \quad \text{(kN)} \tag{23}$$

where D_{WT} is the dead weight of floating vessel (Unit: tonf) and V_o is the impact velocity of floating vessel (Unit: m/s). Comparing of Eq. (3) with Eq. (23), it can be found that two equations are quite similar each other. For both Eq. (3) and Eq. (23), the impact load is proportional to velocity and square root of mass (or weight). Thus, Eq. (23) can be used to determine the impact load when stiffness of submarine is not known.

Duration of impact load is also important factor that affects impact behavior of SRFT. Duration of impact load can be determined by using momentum conservation law. Assuming the submarine stops after collision, following relationship can be obtained as

$$M_{su}V_0 = \int_0^{t_d} F(t)\,dt = \frac{2t_d}{\pi}F_{max} \tag{24}$$

where M_{su} is the total mass of submarine including added mass of water in *kg*, and V_o is the velocity of floating vessel in m/s. From Eq. (24), duration of impact load can be determined as

$$t_d = \frac{\pi}{2}\frac{M_{su}V_0}{F_{max}}. \tag{25}$$

Substituting Eq. (23) into Eq. (25), t_d is given by

$$t_d = \frac{\pi}{238}\frac{M_{su}}{\sqrt{D_{WT}}} \times 10^{-3} \cong 5.39 \times 10^{-4}\sqrt{M_{su}} \quad \text{(Unit: sec).} \tag{26}$$

It should be noted that Eq. (26) is obtained by assuming added mass of water is 50% of the submarine mass and dead weight are equal to 90% of submarine weight (Kawakami *et al*. 1984).

3. Comparison with finite element analysis

Responses of SFRT under submarine collision were theoretically derived in previous section. To verify derived equations, the theoretical evaluations were compared with those from finite element analysis (FEA). General purpose structural analysis program ABAQUS (2010) was used for the analysis. 3D beam and spring elements were used to simulate the SRFT section and mooring line, respectively. Analysis model is shown in Fig. 8. To minimize the end effect, the length of analysis model was selected as long as enough (10 km). Also, to reduce the analysis time, only half model (The length is 5 km) was modeled by using the symmetric properties. Thus, longitudinal displacement and rotation were restrained for the left end (The center of whole model), and vertical displacement at right end (The point where 5 km is far from the center) was restrained.

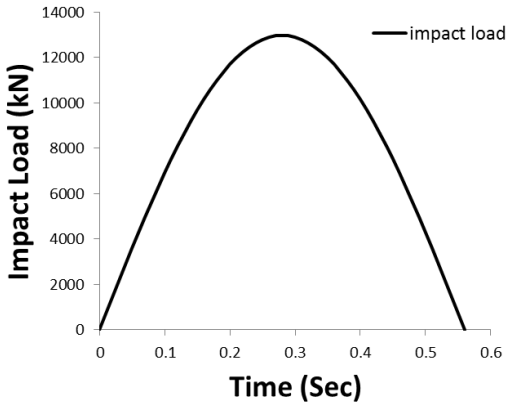

Fig. 9 Applied impact load for FEA

Table 1 Input data for finite element analysis

Description	Value
Young's Modulus, E	2.1×10^{11} N/m^2
Section Area, A	1.7 m^2
Moment of Inertia, I	45.2 m^4
Mass per unit length of SFT including virtual mass, m_s	1.31×10^5 kg/m
Spring Constant, K_s	2.01×10^8 N/m

Discrete mooring lines were modeled as elastic spring where the springs were equally spaced with 100 m span. The impact load was applied at the center of SFRT, as shown in Fig. 8. Applied load is shown in Fig. 9. The detailed section properties of SFRT are adopted from previous research (Seo and Kim 2012) and properties are summarized in Table 1.

Figs. 10 and 11 show the variation in displacement and acceleration with time at the impact point (The center of SFRT), respectively. From the results, it can be found that the maximum displacement from theory and FEA are 67 mm and 66 mm, respectively. The discrepancy between theory and FEA was only 1.5 %. In the case of the maximum acceleration, the difference between theoretical value (1.38 m/s^2) and the results of FEA (1.52 m/s^2) was 9% and the derived equation provided good match with the results of FEA.

The maximum value of displacement and acceleration obtained from derived equations agreed well with the results of FEA. However, the variation in displacement and acceleration with time obtained from theory showed somewhat different behavior with those from FEA, as shown in Figs. 10 and 11. It is because proposed equations were derived based on 1 degree of freedom system with no damping while finite element model had over hundreds of degree of freedom and mode shape. Therefore, overall responses could be different over time. Also, vibration propagated from the center to the end in FEA, as shown in Fig. 12. However, this phenomenon cannot be simulated in one-degree of freedom system. As a result, decrease of peak value shown in FEA was not obtained from the results of theory, as shown in Figs. 10 and 11. It should be noted that the maximum value is more important than time history response for preliminary design of SFRT. Therefore,

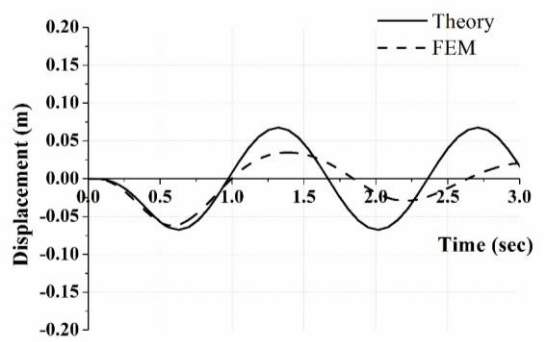

Fig. 10 Comparison of theoretical evaluation with the results of FEA : Displacement

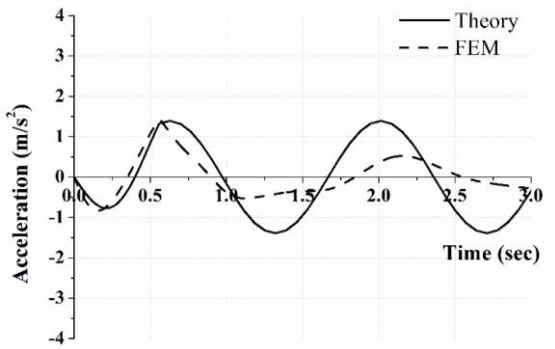

Fig. 11 Comparison of theoretical evaluation with the results of FEA : Acceleration

Fig. 12 Deformed shape of SFRT at 1 sec after collision

proposed equation can provide useful information to design of SFRT.

Bending moment at the center was also compared in this study. Bending moments predicted by theory and FEA were 295,435 kn·m and 212,142 kn·m, respectively. FEA showed 28 % lower bending moment and shows considerable different from theory. It is mainly attributed by accumulation of error from double integration of acceleration. Also, as mentioned before, the theoretical value was derived from 1 degree of freedom model. Thus, the wave propagation may not be properly considered and only one major mode shape is available. The discrepancy between theory and FEA might be occurred from these combined reasons. However, theory gives conservative estimation of bending moment of SFRT and theory could be provided the reference value for preliminary design of the section.

4. Safety assessment for derailment

One of the most important factor that affects safety of railway is derailment. When lateral acceleration is subjected to the section, lateral forces of the wheels which are generated by inertia force of the train and derailment can occur. When lateral and vertical forces of the wheels are

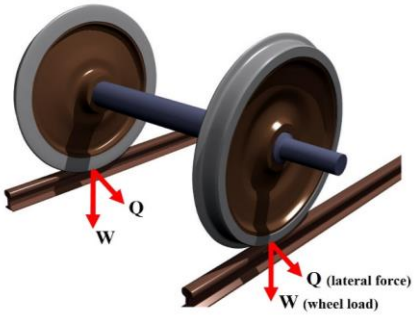

Fig. 13 Wheel rail contact forces

Table 2 Example of derailment evaluation

Description	Value	Applied Eq.
Dead weight of submarine, D_{WT}	1,800 ton	-
Mass of submarine including virtual mass, M_{su}	3,000×10^3 kg	-
Velocity of submarine, V_0	2.56 m/s	-
Collision force, F_c	12,925 kN	Eq. (23)
Impact period, t_d	0.93 sec	Eq. (25)
Effective length, α	65.9 m	Eq. (10)
Distributed mass, m_s	1.31×10^5 kg/m	-
Distributed spring constant, k_s	2.01×10^6 N/m^2	-
Equivalent mass, M_e	1.29×10^7 kg	Eq. (13)
Equivalent spring constant, K_e	2.65×10^8 N/m	Eq. (14)
Natural frequency, ω	4.53 rad/s	-
Frequency ratio	1.34	-
Acceleration ratio, A_{rmax}	1.71	Eq. (22)
Derailment impact force, F_{cd}	59,120 kN	Eq. (31)

known (Refer Fig. 13), the condition for derailment is given by (KRRI 2014)

$$R_d = \frac{Q}{W} < R_{cd} = 0.8 \tag{27}$$

where R_d is the derailment coefficient, Q is the lateral force of the wheel, W is the vertical force of the wheel, and R_{cd} is the critical derailment coefficient. When, R_d is larger than R_{cd} (= 0.8), derailment occurs.

Lateral acceleration due to collision of submarine can be obtained as proposed Eqs. (20) and (22). By using these Eqs. (20), (22) and (27), derailment condition can be written as

$$Q = 0.8W = 0.8gM_v = a_{cd}M_v \tag{28}$$

$$a_{cd} = 0.8g = \frac{F_{cd}\omega^2}{K_e}A_{rmax} \tag{29}$$

$$F_{cd} = 0.8\frac{K_e g}{A_{rmax}\omega^2} = 0.8\frac{M_e g}{A_{rmax}} \tag{30}$$

Where M_v is the vertical mass corresponding to the wheel load, a_{cd} is the critical lateral acceleration and F_{cd} is the critical derailment impact load. Substituting Eq. (13) into Eq. (30), F_{cd} can be rewritten as

$$F_{cd} = 1.2\frac{m_s \alpha g}{A_{rmax}}. \tag{31}$$

The impact load of submarine can be estimated by using Eq. (23) or Eq. (3) when the stiffness of submarine is known. By comparing of impact load of submarine with Eq. (31), safety for derailment of train in SFRT can be assessed. As an example, safety condition for derailment was calculated as shown in Table 2. From the results of Table 2, train was safe for derailment for given SFRT properties, because the collision force was less than the derailment impact force.

5. Conclusions

Behavior of Submerged Floating Railway Tunnel (SFRT) subjected to submarine collision event was evaluated in this study. Based on theory of beam on elastic foundation, impact responses of SFRT, such as displacement, acceleration, and bending moment, were derived. Also, equivalent mass and stiffness were obtained. Derived equations were compared with the results of finite element analysis. From the comparison results, it can be found that the proposed equation gave good prediction of the maximum displacement and acceleration. However, relatively large discrepancy was noted for bending moment prediction, since integration errors are accumulated during calculation. Finally, the condition to assess the safety for derailment of train in SFRT was suggested and calculation example was provided. All proposed equations have simple and closed form. Thus, these equations might be effectively used for preliminary design process of SFRT.

Acknowledgements

This research was supported by a grant from R&D Program of the Korea Railroad Research Institute, Republic of Korea

References

AASHTO (2009), Guide Specifications and Commentary for Vessel Collision Design of Highway Bridges, 2nd Edition.

ABAQUS (2010), Abaqus Analysis User's Manual version 6.10, Dassault Systèmes Simulia Corp.

Consolazio, G., Cowan, D., Biggs, A., Cook, R., Ansley, M. and Bollmann, H. (2005). "Full-scale experimental measurement of barge impact loads on bridge piers", *Tran. Res. Record: J. Tran. Res. Board*, **1936**, 81-93.

DNV (2010), Design Against Accidental Loads, DNV-RP-C204.

Hong, K.W. and Lee, G.H. (2014), "Collision analysis of submerged floating tunnel by underwater navigating vessel", *J. Comput. Struct. Eng. Inst. Korea*, **27**(5), 367-77. (in Korean)

Kanie, S. (2010), "Feasibility studies on various SFT in Japan and their technological evaluation", *Procedia Eng.*, **4**, 13-20.

Kawakami, M. (1984), *Guide to Ship Vibration*, Nippon Kaiji Kyoka.

Korea Railroad Research Institute (KRRI) (2014), Technical Specifications for Urban Railway Vehicles, Ministry of Land & Transport of Korea Government. (in Korean)

Mazzolani, F.M., Faffiano, B. and Matire, G. (2010), "Design aspects of the AB prototype in the Qiandao Lake", *Procedia Eng.*, **4**, 21-33.

Østlid, H. (2010), "When is SFT competitive?", *Procedia Eng.*, **4**, 3-11.
Seo, S.I. and Kim, J.S. (2012), "Simplified collision analysis method using theory of beam with elastic foundation", *2012 Spring Conference Proceedings of Korean Society for Railway*, 559-566. (in Korean)
Ugural, A.C. and Fenster, S.K. (2012), *Advanced Mechanics of Materials and Applied Elasticity*, Prentice Hall, 5th Edition.
Zhang, S., Wang, L. and Hong, Y. (2010), "Vibration behavior and response to an accidental collision of SFT prototype in Qiandao Lake (China)", *Procedia Eng.*, **4**, 189-97.

PL